DEM-MBD Coupled Simulation of a Burrowing Robot in Dry Sand

Sarina Shahhosseini, S.M.ASCE¹; Mohan Parekh²; and Junliang Tao, Ph.D., A.M.ASCE³

¹Graduate Student, School of Sustainable Engineering and the Built Environment, Center for Bio-Mediated and Bio-Inspired Geotechnics, Arizona State Univ., Tempe, AZ.

Email: sshahho1@asu.edu

²Undergraduate Student, Center for Bio-Mediated and Bio-Inspired Geotechnics, Arizona State Univ., Tempe, AZ. Email: maparekh@asu.edu

³Associate Professor, School of Sustainable Engineering and the Built Environment, Center for Bio-Mediated and Bio-Inspired Geotechnics, Arizona State Univ., Tempe, AZ (corresponding author). Email: jtao25@asu.edu

ABSTRACT

This study demonstrates the application of a coupled discrete element method (DEM)—multibody dynamics (MBD) framework in simulating the self-burrowing behavior of a robot in dry sand. In robotics, a robot can be modeled using MBD, in which each component of the robot is modeled as interconnected rigid or flexible bodies whose motions obey the laws of motion and are limited by kinematic constraints. In this study, DEM is coupled to MBD using Chrono—an open-source physics engine—to model the self-burrowing behavior of a two-auger robot in dry sand. The robot consists of a pair of horizontally aligned, auger-shaped bodies, which are connected with two rotational motors in MBD; and the sand is simulated as packing of monodispersed, frictional spheres in DEM. A typical co-simulation loop starts with the DEM module that solves the inter-particle and particle-structure forces and displacements; the particlestructure forces are then transferred to the MBD module to solve the dynamics of the robot; with the updated robot position and velocity, information is then transferred back to the DEM module. The rotation of the augers was set to different directions and speeds. It was found that the rotation of the two augers in the same direction enables horizontal translational movement of the robot, while rotation in the opposite directions hinders such movement: higher rotational speeds lead to higher translational velocities.

INTRODUCTION

Bio-inspired burrowing robotics is an emerging field at the interface of biology, robotics, and soil mechanics. Such robots can find applications in exploration, search and rescue, sensor deployment, inspection, monitoring, surveillance, transport, and construction purposes (Tao 2021). A key question to answer is how a burrowing organism or its robot counterpart moves by itself in the soil. Of interest in this paper is burrowing driven by helical motions such as that used by self-burying seeds (Jung et al. 2014). The awns of these self-burying seeds coil and uncoil in response to the environment's moisture content, resulting in rotation and helical motions. Such a self-burying process is similar to screw driving, auguring or drilling processes but differs in that the motions are self-generated, and no external forces are needed. Previously, this helically driven burrowing process has been modeled using an analytical approach based on Coulomb's friction law with idealized helical geometry and properties of the granular media (Darbois Texier et al. 2017).

To assist robotic design and to better understand robot-granular media interactions, the discrete element method (DEM) is often used (Chen et al. 2022; Huang and Tao 2020; Ma et al. 2020; Tang and Tao 2022). However, most of the simulations were "displacement-controlled", meaning that the simulations were advanced by prescribing the displacement or velocity of the burrowing robot. Therefore, the motion of the robots does not have to obey Newton's laws of motion. In contrast, a robotic structure can be modeled using Multi-body Dynamics (MBD), in which each component of the robot is modeled as interconnected rigid or flexible bodies whose motions obey the laws of motion. The movements of the components can be limited by kinematic constraints such as linear or rotational joints.

In this study, DEM is coupled to MBD using Chrono – an open-source physics engine – to demonstrate the modeling of the self-burrowing behavior of a bio-inspired two-auger robot in dry sand. In such a simulation, the contacts between particles and robot components are detected and the corresponding reaction forces are resolved and shared. The motions of all the particles and robot components are more faithfully modeled since they all obey Newton's laws of motion.

METHODOLOGIES

DEM model. In a DEM simulation, particles are allowed to undergo small interpenetrations, and the primary assumption is that the mechanical behavior of the system is understood by Newtonian dynamic updates between individual entities (Campello 2018). In each time step, the normal contact force, friction tangential force, rolling friction torque and cohesion forces are calculated based on the stiffness, damping coefficients, and contact constitutive models including the Hertzian contact theory, the Mindlin friction law, and rolling resistance models (Fang et al. 2021). The stiffness and damping parameters of the Hertzian model are defined based on material properties, including Young's modulus, Poisson's ratio, and coefficient of restitution.

In Chrono, the DEM part leverages the Graphic Processing Unit (GPU) architecture and is handled by the Chrono::GPU simulator. In Chrono::GPU, a few efficiency-enhancing features are implemented: 1) mixed data types are used to reduce memory footprint and increase simulation speed, and 2) a Lined-Cell based domain decomposition approach and combined global-subdomain particle position representation are implemented to improve memory bandwidth and cache utilization.

The granular material consists of sphere-shaped bodies with a radius of 5 mm and assigned elastic and plastic materials as defined in Table 1. The elastic and plastic material properties are derived from a previous study in which a validation test, using glass bead particles, was performed (Thoesen et al. 2019). Another recent study has been investigated the validation of Project Chrono by performing both laboratory and simulated direct shear test (Yong and Tao 2023).

Robot design and MBD model. MBD allows the modeling of dynamical systems and studies the kinematic updates and constrains between assembled rigid or deformable bodies (Skrinjar et al. 2018). In Chrono, the MBD part is handled by the Chrono core APIs. The MBD module calculates the kinematic updates of the robot based on the contact forces from the granular particles in contact with the robot.

In this study, rigid bodies were first defined, and rotational motor links were then utilized to constrain the motion of the augers. A burrowing robot is designed based on the helically driven burrowing mechanism. The general concept is to generate horizontal translational motion from axial rotation of a helical auger. In practice, a rotational motor must be used to drive the auger

and an anti-torque component is needed to prevent the rotational slip of the robot. That is the auger, and the anti-torque component is connected using a rotational motor link in which the anti-torque component is considered as a stator. The geometry of the augers and stators are shown in Figure 1.

Table 1: Material and interactive properties of the simulated particles and meshes

| Material Property | Particles | Mesh (robot) objects |
|--|-----------|----------------------|
| Particle radius (cm) | 0.15 | - |
| Density (g/cm ³) | 2.55 | 1 |
| Poisson's ratio (-) | 0.22 | 0.3 |
| Young's modulus (Pa) | 7 e7 | 1.8 e9 |
| Interactive Property | Phase 1 | Phase 2 |
| Coefficient of restitution: sphere-sphere | 0.22 | 0.22 |
| Coefficient of restitution: sphere-wall | 0.22 | 0.22 |
| Coefficient of restitution: sphere-mesh | 0.3 | 0.3 |
| Coefficient of static friction: sphere-sphere | 0.08 | 0.16 |
| Coefficient of static friction: sphere-wall | 0.08 | 0.16 |
| Coefficient of static friction: sphere-mesh | 0.15 | 0.3 |
| Coefficient of rolling friction: sphere-sphere | e 0.0 | 2.5 e-5 |
| Coefficient of rolling friction: sphere-wall | 0.0 | 2.5 e-5 |
| Coefficient of rolling friction: sphere-mesh | 0.0 | 0.17 |

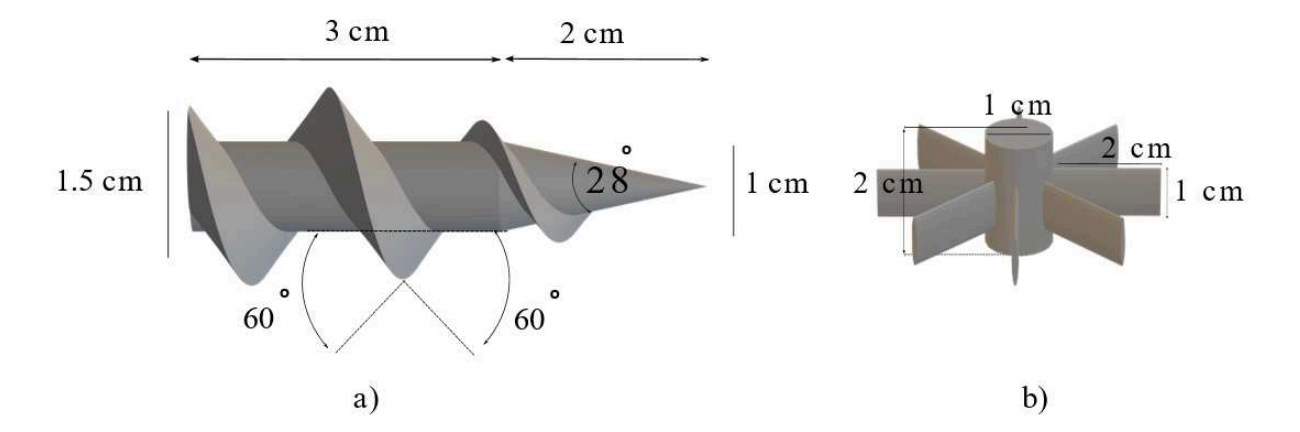


Figure 1: Dimensions of the robotic parts: a) horizontal augers; b) stators

To facilitate dual-directional burrowing, a second set of auger-stator is created as a mirror of the first set, and the two stators are connected using a fixed link (Figure 2).

Co-simulation Workflow. DEM and MBD are incorporated in Chrono:: GPU module, and the sharing and transferring data between DEM and MBD are achieved through a co-simulation workflow (Figure 3). In a nutshell, the Chrono::GPU engine or the DEM module, computes the

contact forces and torques between contacting particles as well as between the robot rigid body meshes and the particles in contact with them. The particle-mesh contact forces and torques are then transferred to the Chrono core module, in which the dynamics of the mesh objects are simulated to update their position and velocity information. These updates are then transferred back to the Chrono::GPU engine to update the dynamics of the granular media.

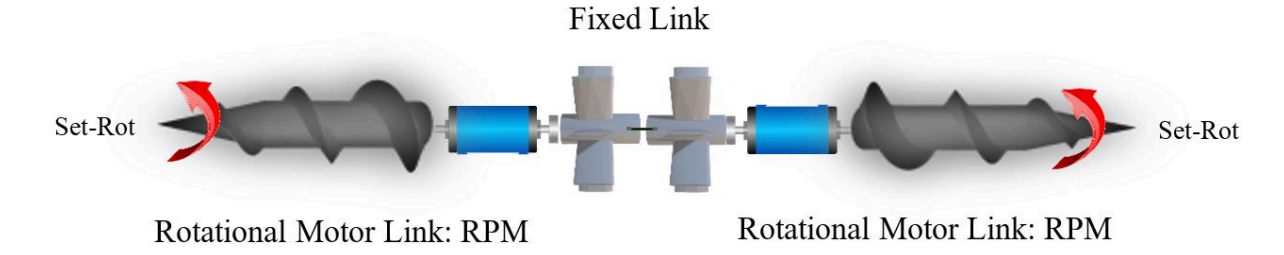


Figure 2: Illustration of the robot assembly and kinematic constraints (rotational motor link and fixed link) among multiple body parts.

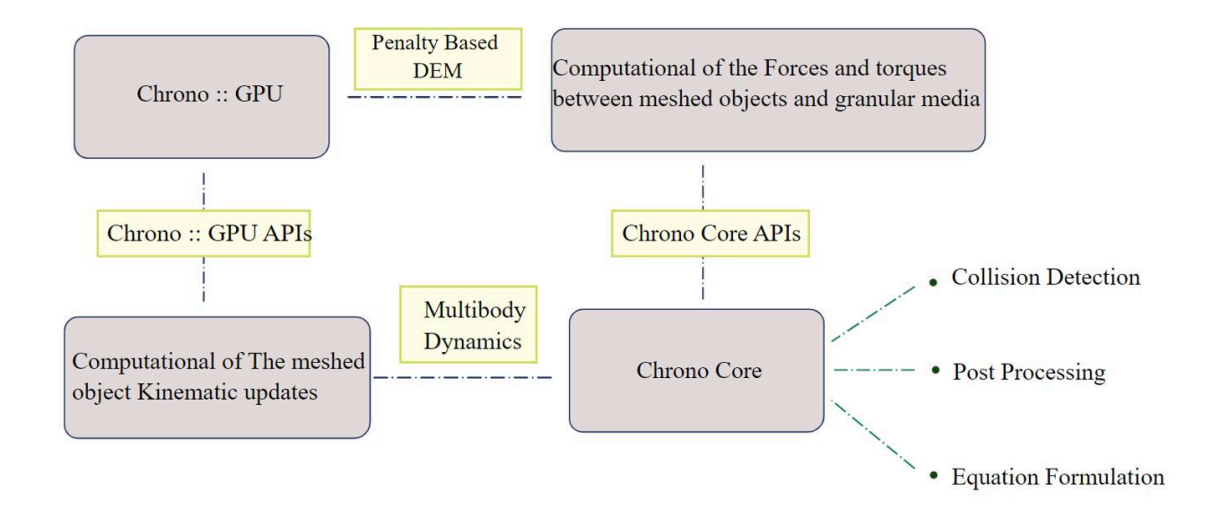


Figure 3: DEM- MBD Co simulation workflow diagram (Fang et al. 2021)

Simulation Set up. The simulations were conducted in two phases. Phase 1 is the model preparation phase, in which two layers of particles (602110 particles) were generated using a disk sampling method with layer distance of 2.04 times of particle radius. The particle layers started from height of 0 to 95 cm and the robotic parts were placed between two sections of particle layers. The particle layers and robotic parts were then allowed to fall by gravity into a big box with width of 42 cm and depth of 26 cm. In Phase 1, lower friction coefficients were used to facilitate particles sliding and rotation, which results in a relatively dense sample with a void ratio of 0.65.

In phase 2, two motors defined by two links (Chrono::ChLinkMotorRotationSpeed) between stators and augers were activated to rotate the horizontal augers. Stators are attached by fixed links (Chrono::ChLinkMateFix). Previous simulations indicated that if stators had no blades, lack of adequate anti-torque would result in rotation of stators instead of the augers in the simulation. Fig. 4 illustrates the packing of the granular media as well as the position of the robot assembly at the beginning of Phase 2.

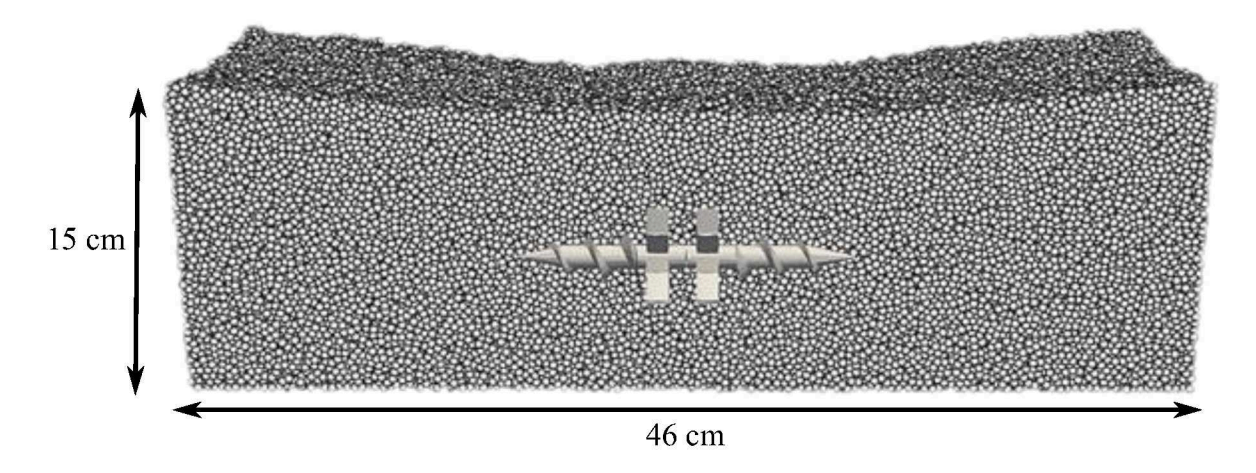


Figure 4: Cross section of simulation set up after sample preparation

Increasing rotation speed of a cone penetrator during vertical penetration has been shown to decrease the resistive force and contact numbers (Tang and Tao 2022). In addition, using augers-shaped penetration instead of a cone and shaft better helps with particle relocating and breaking the geometry and kinematics symmetry, which facilitate the generation of net thrust force for burrowing. As a preliminary study, we studied the effect of the augers' rotational speed and rotational direction on burrowing speed and related thrust and resistance forces during burrowing. Two sets of simulations with rotation speeds of 30, 60, and 90 revolutions per minute (rpm) were conducted. In the first set of tests, the motors rotated the augers around the negative global y-axis, while in the other set, the augers had opposite rotational directions (the left and the right auger had positive torques in local coordinate frame). The local and global axis of each auger is shown in the Figure 5.

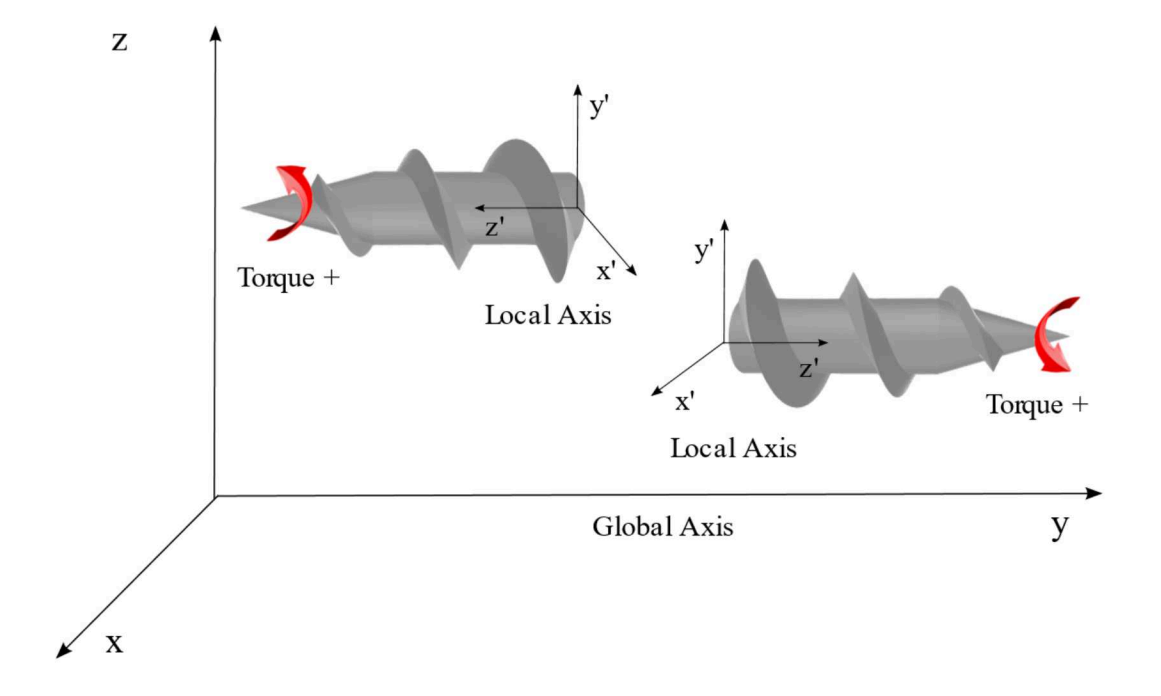


Figure 5: The global axis of the simulation and local axis of the augers

RESULTS

Burrowing displacements. The displacement of the robot was obtained directly from the simulations with different rotational speeds and directions. When the generated torques from the left and right augers are in the same direction (Tr+ and Tl+) due to the same global rotation direction, the horizontal burrowing speed increases with rotational speeds (Figure 6a); there also exist vertical displacements, although much smaller than the horizontal displacements (Figure 6b).

In addition, when the generated torques from the left and right augers are in opposite directions (Tr- and Tl+) due to the opposite global rotation directions, the robot does not have obvious horizontal displacement (Figure 6a) but moves downward slightly (Figure 6b).

For instance, at the same rotational speed of 90 RPM and when augers rotate in the same direction, the robot moves 3.5 cm leftward and 0.2 cm upward in 5 seconds; on the other hand, when augers rotate in opposite directions, the simulation shows almost no vertical displacement for the robot.

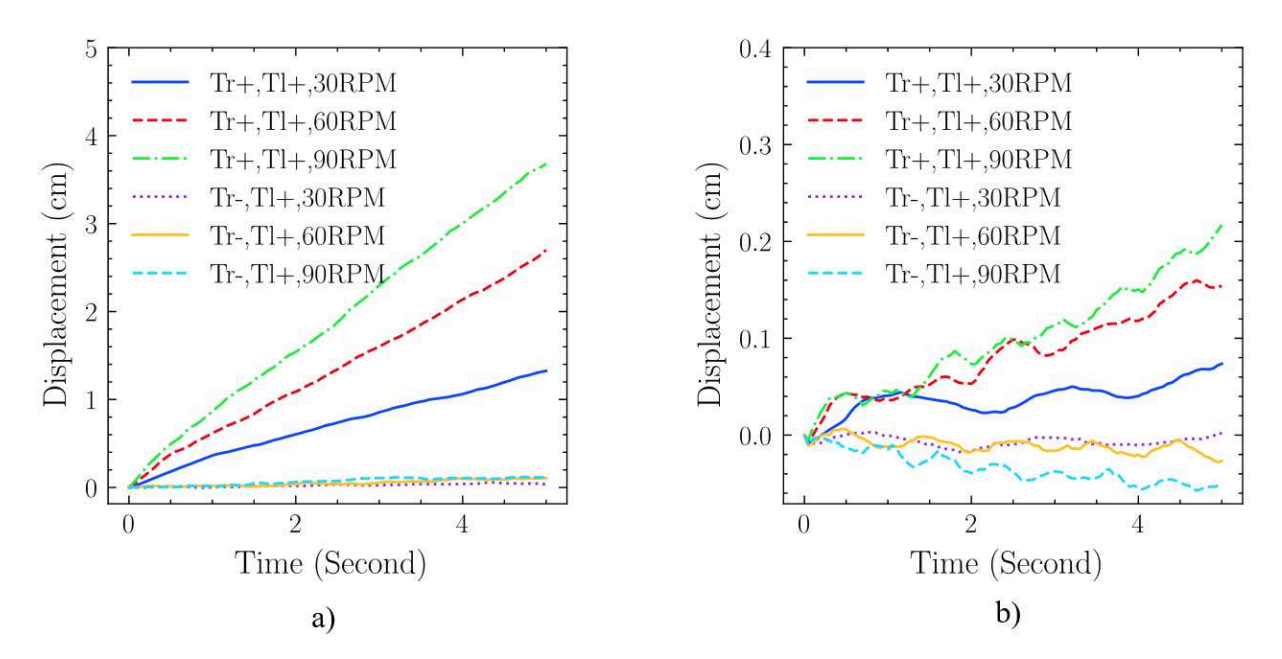


Figure 6: Displacement of the simulated robot (Global axis): a) Horizontal displacement (Zaxis); b) Vertical displacement(Yaxis)

Burrowing forces and torques. The resultant contact forces and torques by particles on auger meshes were obtained and the *Y* -components (horizontal force and clockwise torque) are plotted in Figure 7 and Figure 8, in which L.A and R.A indicate the left and the right auger.

With the same rotational direction, particles generate reaction forces and torques in the same direction on the two augers (Figure 7a and Figure 8a), indicating that both augers contribute to the thrust force which propels the robot forward; the forces and torques on the right auger are consistently lower than those on the left auger, due to the fact that the left auger first interacts with the undisturbed soils while the right auger only interacts with distributed soils.

With opposite rotational directions, particles generate reaction forces and torques in the opposite directions on the two augers (Figure 7b and Figure 8b).

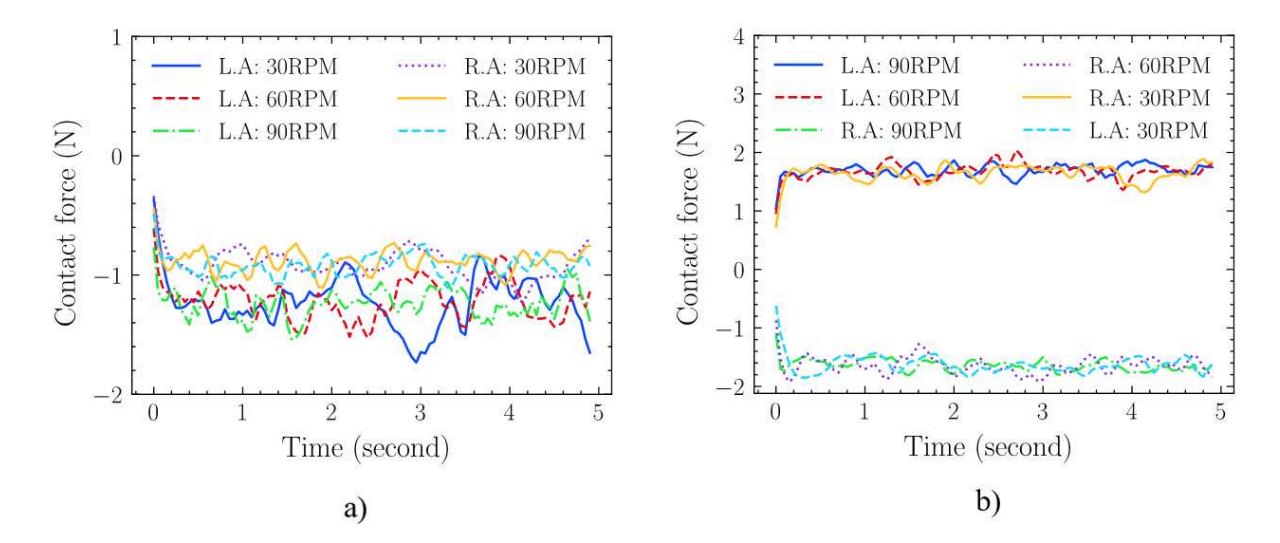


Figure 7: Contact force applied on the simulated robot (Global axis): a) first set in which augers rotate in same directions; b) Second set in which augers rotate in opposite directions

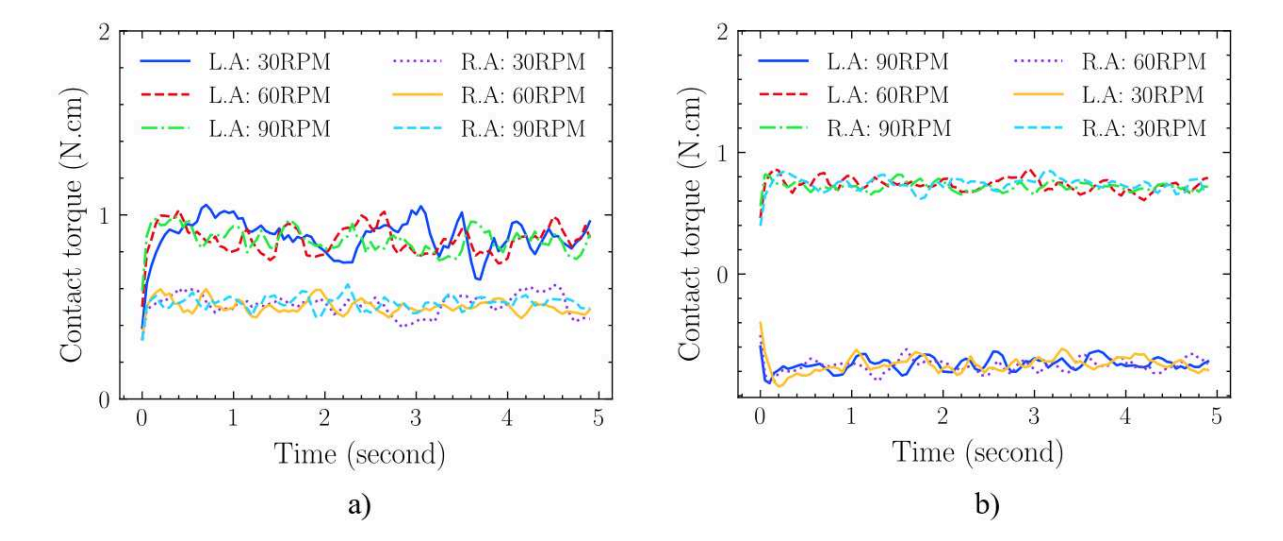


Figure 8: Contact torque applied on the simulated robot (Global axis): a) first set in which augers rotate in same directions; b) Second set in which augers rotate in opposite directions

Also, since the thrusts are in the opposite direction and there is no obvious tendency for the robot to move in either direction, the soil states on the two sides are similar to each other and the magnitudes of the resulting contact forces and contact torques in these two directions are almost identical. In summary, the generated thrusts from the two augers cancel out each other for the most part and the horizontal movements are negligible.

DISCUSSIONS

In all the simulations, vertical movements were observed. For the cases where the rotation directions of the two angers are the same, upward movements are expected due to the phenomenon termed "drag induced lift" (Ding et al. 2011), which is mainly due to the intrinsic

gradient in earth pressure. The vertical force on the top half of the robot is higher than that on the bottom half, resulting in a net lift force driving the robot upward. Also, the rotation of the augers leads to disturbance of the soil around them, and the particles will have a tendency to flow downward due to gravity, filling any available voids at the bottom of the robot. These observations are consistent with the models and findings on the upward burrowing mechanisms of razor clams (Tao et al. 2020).

While the objective of this paper is to demonstrate the capabilities of a DEM-MBD cosimulation tool in modeling the self-burrowing phenomenon, the full potential of such as method was not presented due to the length limitations. In the future, the rich particle-level force data can be used to better understand the burrowing mechanisms; due to the high computational performance of the Chrono::GPU simulator, it can be applied to perform parametric studies to aid the design and control of the burrowing robots.

CONCLUSIONS

In this study, DEM-MBD co-simulations were performed to demonstrate the self- burrowing behaviors of a two-auger robot. Project Chrono, an open-source physics-based platform, was utilized to calculate the contact forces and torques between particles and rigid mesh bodies using DEM and to calculate kinematics updates and complicated constraints in a system of rigid bodies using MBD. The results show that rotational speed and directions of the two augers with the same hardness directly affect its burrowing behavior. Specifically, when the rotation directions of the two augers are the same, both augers generate thrust in the same direction, and both contribute to the horizontal movement of the robot; the burrowing speed increases with the rotational speeds. On the other hand, when the rotation speeds are the same but the rotation directions of the two augers are opposite, the thrusts generated from the two augers cancel out each other and no translational movements are observed. In summary, it is concluded that DEM - MBD co-simulations can be applied to model robotic burrowing in granular media.

ACKNOWLEDGEMENT

This material is based upon work supported by the National Science Foundation (NSF) under NSF CMMI 1849674 and CMMI 1841574. Any opinions, findings, and conclusions or recommendations expressed in this material are those of the authors and do not necessarily reflect those of the NSF

REFERENCES

- Campello, E. M. B. 2018. "A computational model for the simulation of dry granular materials." *International Journal of Non-Linear Mechanics*, 106: 89–107.
- Chen, Y., A. Martinez, and J. T. DeJong. 2022. "DEM study of the alteration of the stress state in granular media around a bio-inspired probe." *Can. Geotech. J.*, cgj-2021-0260.
- Darbois Texier, B., A. Ibarra, and F. Melo. 2017. "Helical Locomotion in a Granular Medium." *Phys. Rev. Lett.*, 119 (6): 068003.
- Fang, L., R. Zhang, C. Vanden Heuvel, R. Serban, and D. Negrut. 2021. "Chrono::GPU: An Open-Source Simulation Package for Granular Dynamics Using the Discrete Element Method." *Processes*, 9 (10): 1813. Multidisciplinary Digital Publishing Institute.

- Huang, S., and J. Tao. 2020. "Modeling Clam-inspired Burrowing in Dry Sand using Cavity Expansion Theory and DEM." *Acta Geotech.*, 15 (8): 2305–2326.
- Huang, S., and J. Tao. 2022. "Bioinspired Horizontal Self-Burrowing Robot." *Geo-Congress* 2022, 223–231. Charlotte, North Carolina: American Society of Civil Engineers.
- Jung, W., W. Kim, and H.-Y. Kim. 2014. "Self-burial Mechanics of Hygroscopically Responsive Awns." *Integrative and Comparative Biology*, 54 (6): 1034–1042.
- Lommen, S., D. Schott, and G. Lodewijks. 2014. "DEM speedup: Stiffness effects on behavior of bulk material." *Particuology*, 12: 107–112.
- Ma, Y., T. M. Evans, and D. D. Cortes. 2020. "2D DEM analysis of the interactions between bio-inspired geo-probe and soil during inflation-deflation cycles." *Granular Matter*, 22 (1): 11.
- Mazhar, H., T. Heyn, A. Pazouki, D. Melanz, A. Seidl, A. Bartholomew, A. Tasora, and D. Negrut. 2013. "CHRONO: A parallel multi-physics library for rigid-body, flexible-body, and fluid dynamics." *Mech. Sci.*, 4 (1): 49–64.
- Skrinjar, L., J. Slavič, and M. Boltežar. 2018. "A review of continuous contact-force models in multibody dynamics." *International Journal of Mechanical Sciences*, 145: 171–187.
- Tang, Y., and J. Tao. 2021. Effect of Rotation on Penetration: Toward a Seed Awn-Inspired Self-Burrowing Probe. 149–159. American Society of Civil Engineers.
- Tang, Y., and J. Tao. 2022. "Multiscale analysis of rotational penetration in shallow dry sand and implications for self-burrowing robot design." *Acta Geotech*.
- Tao, J. 2021. "Burrowing soft robots break new ground." *Science Robotics*, 6 (55). Science Robotics.
- Thoesen, A., T. McBryan, and H. Marvi. 2019. "Helically-driven granular mobility and gravity-variant scaling relations." *RSC Adv.*, 9 (22): 12572–12579.
- Yong, T., and J. Tao. 2023. "Comparative Analysis of Horizontal Self-burrowing Strategies using Full-scale DEM-MBD Co-simulations", submitted, *GeoCongress* 2023.